Crack Systems in Multiaxial Fatigue

D. L. McDIARMID
Department of Mechanical Engineering and Aeronautics, City University, London EC1V 0HB, UK

ABSTRACT

The results of biaxial fatigue tests on thin wall steel cylinders covering a range of principal stress amplitude ratio, out-of-phase angle and frequency ratio are reported and discussed. Four different types of crack growth behaviour have been identified in these tests, depending on the state of multiaxial stress existing. Uniaxial push-pull fatigue test data cannot be used as being generally representative of multiaxial fatigue stress conditions. Each particular type of crack growth behaviour can be correlated by the Tresca shear stress criterion of failure.

KEYWORDS

Biaxial and multiaxial fatigue; biaxial crack propagation; life assessment; principal stress ratio; out-of-phase cyclic loading; frequency ratio; cumulative damage; anisotropy.

NOMENCLATURE

α	Frequency ratio = frequency of σ_{2a}/frequency of σ_{1a}.
λ	Principal stress amplitude ratio = σ_{2a}/σ_{1a}.
ϕ	Out of phase angle, where σ_2 leads σ_1; related to σ_2 where 1 cycle of σ_2 is 360°.
σ_1, σ_2, σ_3	Principal stresses ($\sigma_1 > \sigma_2 > \sigma_3$).
σ_{1a}, σ_{2a}, σ_{3a}	Principal stress amplitudes.
σ_a	Stress amplitude.
σ_n	Normal stress amplitude on the plane of maximum range of shear stress.

τ	Shear stress amplitude.
$\tau_{12}, \tau_{23}, \tau_{31}$	Shear stress amplitudes on the 12, 23, 31 planes of maximum range of shear stress.
τ_a	Shear stress amplitude on the plane of maximum range of shear stress.
12, 23, 31	Planes of maximum range of shear stress associated with the 1, 2, 3 principal stress directions.
1, 2, 3	Longitudinal, transverse (hoop) and radial directions respectively.

INTRODUCTION

Despite over one hundred years of research experience it is still not possible to prevent the failure of components in service due to fatigue. Many components in service are subjected to complex multi-axial fatigue stress conditions which make it very difficult to assess how fatigue damage occurs and how this damage accumulates during the life of the component. Common examples of fatigue under multiaxial stress are axles, crank shafts and propellor shafts subjected to combined bending and twisting which can be out of phase and at different frequencies. Pressure vessels and piping are other examples and many notches and geometric discontinuities are subject to such complex stress situations. Many attempts have been made to derive theories which can cope with these complex multiaxial fatigue stress situations based on simple laboratory test data such as the uniaxial reversed stress fatigue test. A large number of theories of multiaxial fatigue have been proposed and many are reviewed in references (Brown and Miller, 1973; Garud, 1981).

The author has, amongst others, proposed (McDiarmid, 1972, 1973) that the important parameters for long life fatigue in the unnotched situation are the alternating and mean stresses, both normal and shear, occurring on the plane of maximum range of shear stress. This theory has been extended for the case of out-of-phase biaxial stresses (McDiarmid, 1977, 1981) where it is shown that the out-of-phase stresses produce shorter fatigue lives than equal in-phase stresses. A further extension of this work (McDiarmid 1985) has been carried out for the case where the biaxial stresses are not only out-of-phase but also at different frequencies.

A recent paper (McDiarmid, 1988) describes the results of further tests conducted under similar conditions to those in (McDiarmid, 1985), in an attempt to firstly consolidate the tentative conclusions of the earlier work and secondly to extend the investigation of the out-of-phase cases to include the effect of mean stress.

A continuation of the work reported in (McDiarmid, 1988) has led to the realisation that a number of different cracking systems are operating, depending on the particular multiaxial fatigue stress system being applied, and that these cracking systems require to be investigated in more detail. The present paper describes this work.

CRACK SYSTEMS IN MULTIAXIAL FATIGUE

Brown and Miller (1973) have shown that there are two possible cases of crack growth under biaxial fatigue conditions. Case A arises for negative values of $\lambda = \sigma_2/\sigma_1$ (actually σ_3/σ_1) where the cracks propagate along the

surface and the surface strains are ε_1 and ε_3 as shown in Fig. 1. Case B arises for positive value of $\lambda = \sigma_2/\sigma_1$ where the cracks propagate inwards and the surface strains are ε_1 and ε_2 as shown in Fig. 1. Case B is more severe than Case A.

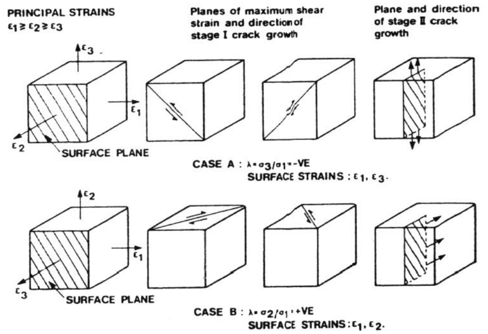

Fig. 1. Planes of maximum shear and crack growth direction [From (Brown and Miller, 1973)]

Following Miller and Brown (1985) the three possible Stage I and Stage II cracking systems can be illustrated as shown in Fig. 2. As the test system used in the present work subjects thin wall tubes to longitudinal load and differential pressure across the wall thickness, the 1,2,3 principal stresses are related to the longitudinal (L,1), hoop (H,2) and radial (R,3) directions. Thus the τ_{12} shear stress system causes Case A Stage I and II cracks growing along the surface. The τ_{23} and τ_{31} shear stress systems cause Stage I cracks growing inwards from the surface and Stage II cracks growing either parallel to the surface or inwards from the surface. The latter cracks are Case B which are the more dangerous.

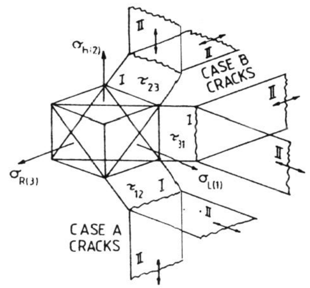

Fig. 2. Crack growth planes and directions

EXPERIMENTAL PROGRAMME

A series of fatigue tests were carried out on thin-wall tubular specimens subjected simultaneously to constant amplitude alternating longitudinal load and alternating differential pressure across the wall thickness. These tests covered the range of principal stress amplitude ratio, out-of-phase angle and frequency ratio shown in Table 1. Note that in the testing $\sigma_1 = \sigma_{longitudinal}$ and $\sigma_2 = \sigma_{transverse}$ (hoop), the frequency of σ_{2a} was the greater and equalled 30 Hz in the tests conducted.

Table 1. Test conditions. For all tests, σ_1 is longitudinal and σ_2 is transverse.

Case	$\lambda = \sigma_{2a}/\sigma_{1a}$	ϕ = Phase Angle	$\alpha = \dfrac{\text{Frequency of } \sigma_{2a}}{\text{Frequency of } \sigma_{1a}}$
1	0	(longitudinal stress only)	
2	$\frac{1}{4}$	0	1
3	$\frac{1}{2}$	0	1
4	$\frac{3}{4}$	0	1
5	1	0	1
6	2	0	1
7	∞	(transverse stress only)	
8	$\frac{1}{2}$	180°	1
9	1	180°	1
10	2	180°	1
11	3	180°	1
12	1	0	2
13	1	90	2
14	1	0	3
15	1	180	3

MATERIAL AND SPECIMEN

The material used in this investigation was EN 24 T steel. The nominal material chemical composition is detailed in (McDiarmid, 1985). The minimum specification mechanical properties were: tensile strength 850 MN/m², yield strength 680 MN/m² and elongation 18%. The specimen dimensions are shown in Fig. 3. The test section outside diameter was produced with a fine turned finish and the inside final diameter was obtained by honing. The wall thickness of 0.635 mm used was a compromise between buckling instability problems and the magnitude of the pressure required to produce fatigue failure.

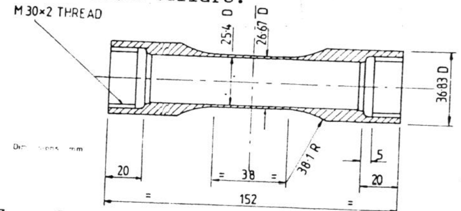

Fig. 3. Specimen geometry and dimensions.

TEST EQUIPMENT

The thin wall tubular specimen was mounted in a pressure test cell device, shown in Fig. 4. capable of producing a differential pressure across the wall thickness. The device was then assembled in a standard 250 kN Schenck fatigue test machine. The complete test system is described in (McDiarmid, 1985). It is relevant to note that the bore and annular areas of the specimen subject to pressure were arranged to be equal. Hence a constant tensile longitudinal stress (regardless of the value of the differential pressure applied across the wall thickness) due to the

pressure, acted on the thin wall section of the specimen, but this could be offset if required, by an actuator load in order to obtain only an alternating differential pressure with no longitudinal stress.

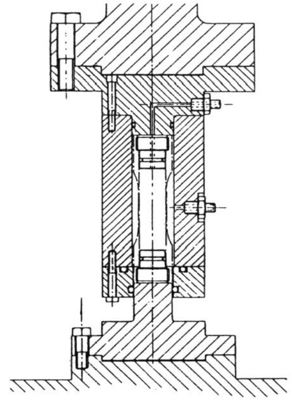

Fig. 4. The pressure test cell.

CRITICAL SHEAR PLANES AND CRACK GROWTH PLANES AND DIRECTIONS

The critical shear planes and crack growth planes and directions for the in-phase cases 1 to 7, that is for $\lambda = 0, \frac{1}{4}, \frac{1}{2}, \frac{3}{4}, 1, 2$ and α, are shown in Fig. 5. with comments, and for the 180° out-of-phase cases 8 to 11, that is for $\lambda = \frac{1}{2}$, 1, 2 and 3 in Fig. 6 with comments. The cases 12 to 15 where the stresses are at different frequencies are discussed separately later. Table 2 summarises crack information for cases 1 to 12, from Figs. 5 and 6. Table 3 gives the values of the shear and normal stresses acting on the critical shear planes for cases 1 to 11 in terms of the applied longitudinal stress amplitude, or in terms of the applied hoop stress amplitude in case 7 where only hoop (transverse) stress is applied.

TEST RESULTS AND DISCUSSION

Cases 1 to 7:

Test results for the in-phase cases 1 to 7 are shown in Fig. 7. plotted on a shear stress amplitude basis. Table 2 indicates that we might except three different types of crack growth behaviour for these tests, case 1 ($\lambda = 0$) longitudinal stress only producing transverse cracks of the A/B type with a circular crack front growing into the surface through thickness as distinct from case 7 ($\lambda = \infty$) transverse stress only producing longitudinal cracks of type B growing into the surface through thickness. Cases 2, 3 and 4 ($\lambda = \frac{1}{4}$, $\frac{1}{2}$ and $\frac{3}{4}$) produce a third type of crack growth of transverse cracks of type B growing into the surface through thickness. Cases 5 and 6 (λ = 1 and 2) produce cracks of the same type as for Case 7 ($\lambda = \infty$), transverse stress only. This is substantiated by the test results which show similar results for cases 5, 6 and 7.

For case 1, longitudinal stress only, test results for specimens tested within the pressurised test cell are slightly higher than those produced when the specimen is cycled under longitudinal stress only, but without being in the pressure cell. It is interesting to note that the results of cases 2 ($\lambda = \frac{1}{4}$) and 3 ($\lambda = \frac{1}{2}$) are higher than those of case 1 ($\lambda = 0$).

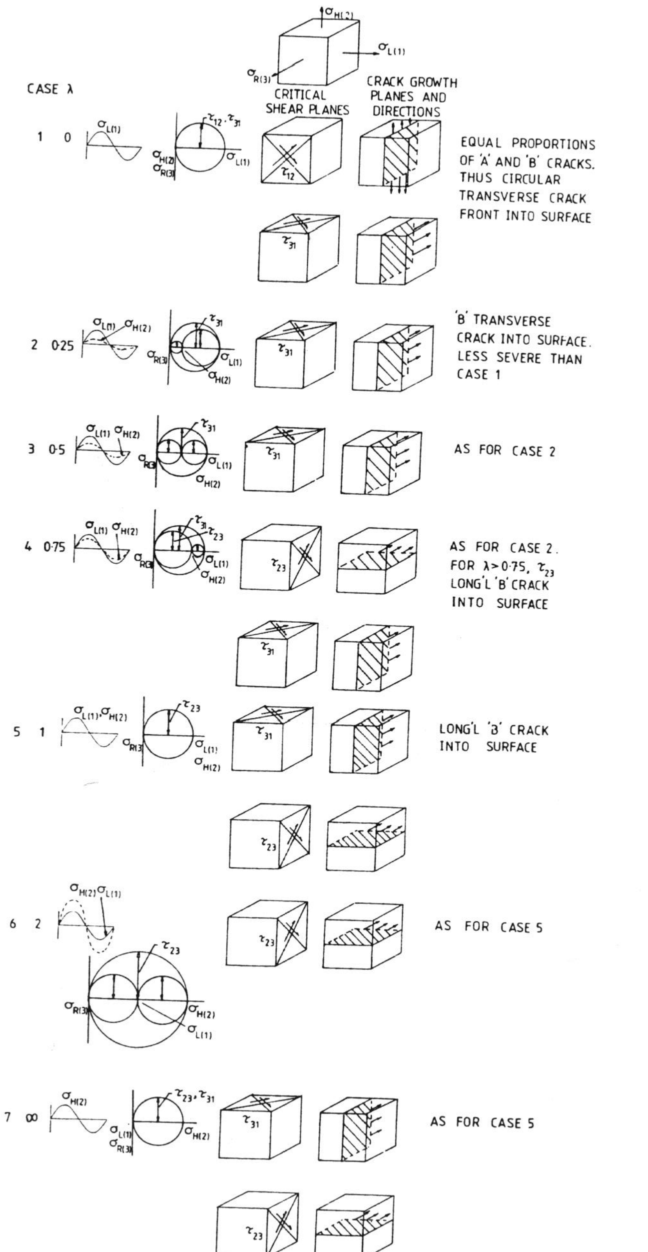

Fig. 5. Critical shear planes and crack growth planes and directions for Cases 1 to 7.

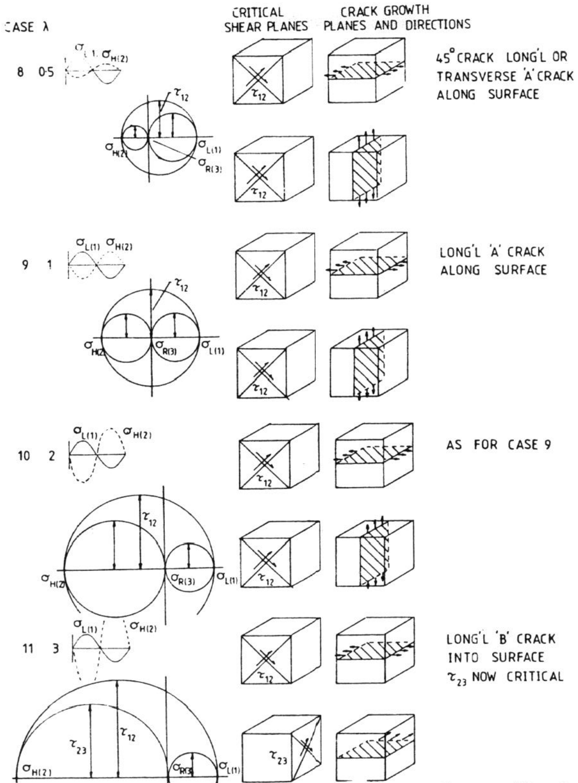

Fig. 6. Critical shear planes and crack growth planes and directions for Cases 8 to 11.

This is because the type A/B circular front crack is more severe than the type B crack and a small transverse stress produces this change in type of crack growth. The case 4 ($\lambda = \frac{3}{4}$) is on the borderline between the transverse type B crack and the longitudinal type B crack, both into the surface through thickness. This case produced cracks of a curved transverse/longitudinal type.

Previous tests (McDiarmid, 1972; Morikawa and Griffiths, 1945; Marin and Shelson, 1949; Ros and Eichinger, 1950; Marin and Hughes, 1952; Rotvel, 1970) of this type using thin cylinders subjected to repeated longitudinal and transverse stress include a mean stress effect and few tests have been conducted in the $\lambda = 0$ to 1 range. Such tests have indicated both higher and lower fatigue strengths and are discussed in (Garud, 1981; McDiarmid, 1972).

The results of transverse stress only fatigue tests on thin wall tubes have often produced much lower fatigue strengths than tests under longitudinal stress only (McDiarmid, 1972; Morikawa and Griffiths, 1945; Marin and Shelson, 1949; Ros and Eichinger, 1950; Marin and Hughes, 1952; Rotvel, 1970). This difference has been adjudged, in the past, to be due to

Table 2. Crack information for Case 1 to 11.

Case	λ	Critical Shear Plane	Crack Type
	$\phi = 0^o$:-		
1	0	12 = 31	Transverse A/B, circular into surface
2	$\frac{1}{4}$	31	Transverse B, into surface
3	$\frac{1}{2}$	31	Transverse B, into surface
4	$\frac{3}{4}$	31	Transverse B, into surface
5	1	23	Longitudinal B, into surface
6	2	23	Longitudinal B, into surface
7	∞	23	Longitudinal B, into surface
	$\phi = 180^o$:-		
8	$\frac{1}{2}$	12	Longitudinal/Transverse A, along surface
9	1	12	Longitudinal A, along surface
10	2	12	Longitudinal A, along surface
11	3	23	Longitudinal B, into surface
	Variety of crack types:-		
	0	12 = 31	Transverse A/B, Circular into surface)
	$0 < \lambda < \frac{3}{4}$	31	Transverse B, into surface)$\phi=0^o$
	$> \frac{3}{4}$	23	Longitudinal B, into surface)
	1, 2	12	Longitudinal A, along surface)
	$\geqslant 3$	23	Longitudinal B, into surface)$\phi=180^o$

material anisotropy whereas it is probably due more to the different types of crack growth occurring. In the present work the transverse fatigue strength is found to be about 75% of the longitudinal strength. Metallurgical examination of transverse and longitudinal sections of the material shows little difference in the material structure, tending to support the argument for anisotropic behaviour of the material being due to different types of crack growth caused by particular three dimensional stress conditions rather than by actual material anisotropy. Tensile tests of small specimens showed the material to be about 8% weaker in the transverse direction compared to the longitudinal direction.

It is also pertinent to note that considerable success has been achieved (McDiarmid, 1972, 1973) in correlating the results of combined bending and twisting fatigue test data on the basis of a shear stress failure criterion modified for the effect of normal stress occurring on the plane of maximum range of shear stress regardless of any material anisotropy occurring. In all cases of combined bending and twisting fatigue the same type A cracks are produced. Similar success has not been achieved (McDiarmid, 1988) in trying to extend the use of the same criterion of failure to the range of test results produced using thin wall cylinders subjected to longitudinal stress and differential pressure, where we have illustrated that a number of different types of crack growth behaviour can occur.

Table 3. Stresses on the critical shear planes for Cases 1 to 11.

Case	λ	Critical Shear Plane	$\frac{\tau_a}{\sigma_{1a}}$	$\frac{\sigma_n}{\sigma_{1a}}$	Applied Stress Amplitudes at 10^6 cycles, MN/m² Long'l(σ_{1a})	Trans(σ_{2a})	Critical Shear Stress Amplitude at 10^6 cycles, MN/m²	Crack Type and Direction
	$\phi = 0^o$:-							
1	0	21,31	0.5	0.5	465	0	230	A/B Transverse
2	$\frac{1}{4}$	31	0.5	0.5	525	131	260	B Transverse
3	$\frac{1}{2}$	31	0.5	0.5	500	250	250	B Transverse
4	$\frac{3}{4}$	23(31)	0.38(0.5)	0.38(0.5)	465	350	230	B Long'l/Trans
5	1	23	0.5	0.5	350	350	175	B Long'l
6	2	23	1	1	180	365	180	B Long'l
7	∞	23	$0.5\sigma_{2a}$	$0.5\sigma_{2a}$	0	350	175	B Long'l
	$\phi = 180^o$:-							
8	$\frac{1}{2}$	12	0.75	0.25	400	200	300	A Long'l
9	1	12	1	0	280	280	280	A Long'l
10	2	12	1.5	0.5	170	340	255	A Long'l
11	3	23	1.5	1.5	110	330	165	B Long'l

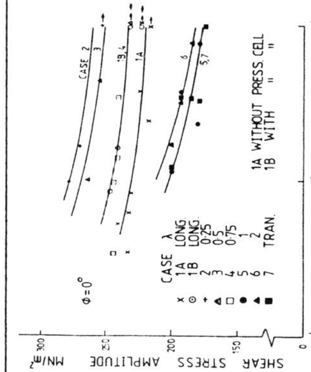

Fig. 7. Test Results. Cases 1 to 7.

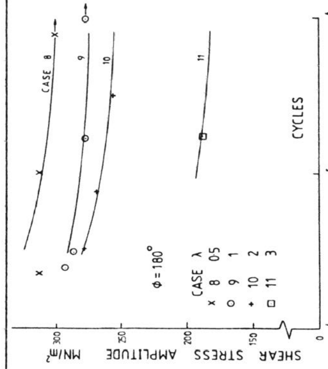

Fig. 8. Test Results. Cases 8 to 11.

Cases 8 to 11:

Test results for the 180° out-of-phase cases 8 to 11 are shown in Fig. 8 again plotted on a shear stress amplitude basis. In some cases only a few failed test results are shown, as buckling difficulties were experienced at the higher stress levels and non-failure at the lower stress levels but the region of the S-N curves is shown with some confidence.

Table 2 indicates that we might expect type A longitudinal cracks growing along the surface through thickness for cases 9 (λ = 1) and 10 (λ = 2). From Table 3, on a shear stress criterion of failure we would expect case 10 to be about 2/3 the fatigue strength of case 9 which is confirmed by the test results. For case 11 (λ = 3) table 2 indicates type B longitudinal cracks growing into the surface through thickness. Type B cracks being more severe than type A cracks we would expect case 11 (λ = 3) fatigue strength to be less than case 10 (λ = 2) even although the normal stress on the critical shear stress plane, which has a secondary effect on the fatigue strength is greater. This is in fact found to be so as shown in Fig. 8. Case 11 (λ = 3, ϕ = 180°) is subjected to the same longitudinal type B cracks as cases 5 (λ = 1, ϕ = 0°), 6 (λ = 2, ϕ = 0°) and 7 ($\lambda = \infty$) thus we would expect the same fatigue strength, as is shown from test results in Figs. 7. and 8.

If case 8 ($\lambda = \frac{1}{2}$) is subjected to the same type A longitudinal cracking as case 9 (λ = 1) we would expect the fatigue strength of case 8 to be about 4/3 the fatigue strength of case 9, that is in inverse proportion to shear stress amplitudes. Test results for case 8, as shown in Fig. 8., indicate that the fatigue strength is somewhat greater than the 4/3 ratio. The test crack is found to be at 45° to the axis of the specimen and it is possible that both τ_{12} and τ_{31} cracking is occurring as $\tau_{31} = 2/3.\tau_{12}$ as shown in Fig. 6.

Case 12 to 15:

Test results for cases 12 to 15 are shown in Fig. 9. plotted on a maximum shear stress amplitude basis.

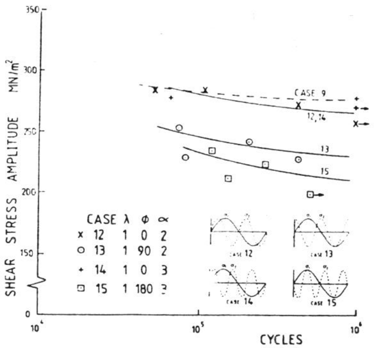

Fig. 9. Test results. Cases 12 to 15.

It has been shown in (McDiarmid, 1985) that when biaxial principal stresses of the same amplitude, but of different frequency, are applied the frequency difference causes the critical shear stress and associated normal stress on the same plane to have varying amplitudes and thus there is a cumulative damage problem. It is also clear that these stresses are out of phase.

For each cycle of σ_{1a} we obtain a number of cycles of τ_{12} and σ_{n12} of different amplitude depending on the value of the frequency ratio. Values of τ_{12} and σ_{n12} for cases 12 to 15, taken from (McDiarmid, 1985) are shown in Table 4. For both shear and normal stresses, only the cycles of greatest amplitude are considered to be damaging. In all of cases 12 to 15 longitudinal type A cracks growing along the surface through thickness occur.

Table 4. Stresses on the critical shear planes for Cases 12 to 15.

Case	Long'l Stress σ_{1a}, at 10^6 cycles, MN/m²	τ_a / σ_{1a}	τ_n / σ_{1a}	Critical Shear Stress Amplitude τ_{12}, at 10^6 cycles, MN/m²
12	294	0 ± 0.88	0 ± 0.88	259
		0 ± 0.18	0 ± 0.18	
13	294	0 ± 0.78	-0.12 ± 0.78	230
		0.28 ± 0.28	0.28 ± 0.28	
14	270	0 ± 1.00	0 ± 0.76	270
		0 ± 0.26	0.38 ± 0.38	
		0 ± 0.26	-0.38 ± 0.38	
15	270	0 ± 0.76	0 ± 1.00	205
		0 ± 0.38	0 ± 0.26	
		0 ± 0.38	0 ± 0.26	
9	278	0 ± 1.0	0	278

Assuming that only the cycles of greatest shear stress amplitude are damaging and neglecting any effect of the normal stress acting on the plane of greatest shear stress amplitude we can compare, on a shear stress criterion of failure, the experimental results for cases 12 to 15 with those of case 9 (λ = 1, ϕ = 180°, α = 1) which have the same longitudinal type A cracks growing along the surface through thickness. This comparison is shown in Table 4, where we see that agreement is reasonable for cases 12 and 14 where the lesser shear stress amplitudes are less than 25% of the greater. In cases 13 and 15 agreement is not good and some allowance has to be made for the damaging effects of the lesser shear stress amplitudes which are 35% and 50% of the greater shear stress amplitudes in cases 13 and 15 respectively.

All cases 1 to 15:

Test results for all cases 1 to 15 are shown in Fig. 10 plotted on the basis of shear stress amplitude at 10^6 cycles versus λ. This tends to indicate three separate bands of results, each consisting of the same type of crack growth behaviour, relative to longitudinal stress only case 1.

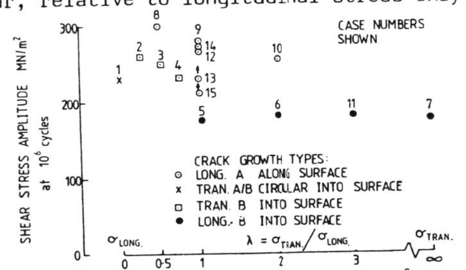

Fig. 10. Shear stress amplitude at 10^6 cycles v λ.

The highest fatigue strengths are found for longitudinal type A along the surface cracks (cases 8, 9 and 10 and also the different frequency cases 12 to 15 should be higher as already discussed), followed by transverse type B into the surface cracks (cases 2 to 4). Both of these crack type bands are greater than the longitudinal stress only case 1. The longitudinal type B into the surface cracks (cases 5 to 7 and 11) form a distinctly lower fatigue strength band relative to the other bands of results.

It is clear that the longitudinal stress only case test results can not be used for general multiaxial fatigue strength prediction as this investigation shows fatigue strength differences of ±25%, using a shear stress criterion of failure, depending on the particular type of crack growth behaviour occurring.

CONCLUSIONS

1. In multiaxial fatigue it is essential to relate the three dimensional cyclic stress state to the characteristics of crack growth, as well as to note any material anisotropy existing.
2. Four different types of crack growth behaviour have been identified in these investigations, dependent on the states of multiaxial stress existing.
3. Uniaxial push-pull fatigue test data can not be used as being representative of multiaxial fatigue stress conditions.
4. The Tresca shear stress criterion of failure is appropriate for correlating each particular type of crack growth behaviour.

ACKNOWLEDGEMENTS

The author gratefully acknowledges the support of the Science and Engineering Research Council.

REFERENCES

Brown, M.W. and Miller, K.J. (1973). A theory for fatigue under multiaxial stress-strain conditions. Proc. Instn. Mech. Engrs., 187, 65/73, 745-755.
Garud, Y.S. (1981). Multiaxial fatigue:A survey of the state of the art. J. Test. Eval., 9, 165-178.
Marin, J. and Shelson, W. (1949). Biaxial fatigue strength of 24S-T aluminium alloy. N.A.C.A. T.N. 1889.
Marin, J and Hughes, W.P. (1952). Fatigue strength of 14S-74 aluminium alloy under biaxial tensile stress. N.A.C.A. T.N. 2704.
McDiarmid, D.L. (1972). Failure criteria and cumulative damage in fatigue under multiaxial stress conditions. P h.D. Thesis, City University, London.
McDiarmid, D.L. (1973). A general criterion of fatigue failure under multiaxial stress. Proc. Int. Conf. Press. Vessel Tech., A.S.M.E., 851-862.
McDiarmid, D.L. (1977). A criterion of fatigue failure under out-of-phase multiaxial stresses. Proc. Can. Cong. App. Mech., 245-246.
McDiarmid, D.L. (1981). Fatigue under out-of-phase bending and torsion. Aero. J. of R. Ae.S., 118-122.
McDiarmid, D.L. (1985a). Designing for high cycle biaxial fatigue using surface strain records. A.S.T.M. S.T.P. 853, 431-439.
McDiarmid, D.L. (1985b). Fatigue under out-of-phase biaxial stresses of different frequencies. A.S.T.M. S.T.P. 853, 606-621.
McDiarmid, D.L. (1988). The effect of mean stress on biaxial fatigue where the stresses are out-of-phase and at different frequencies.

Proc. Second Int. Conf. Multiaxial Fat., to be published.
Miller, K.J. and Brown, M.W. (1985). Multiaxial fatigue : a brief review In:Advances in Fracture Research (P.R. Rao, J.F. Knott and R. Dukey, Ed.). Pergamon, 31-56.
Morikawa, G.K. and Griffiths, L.V. (1945). Biaxial fatigue strength of low carbon steels. Weld. J. Res. Supp., 167-174.
Ros, M. and Eichinger, A. (1950). Die bruchgefahr fester korper bei widerholter beanspruchung ermudung. Metalle, Bericht 173.
Rotvel, F. (1970). Biaxial fatigue tests with zero mean stresses using tubular specimens. Int. J. Mech. Sc., 12, 597-613.